

Facile Synthesis, Diffused Reflectance Spectroscopy & Fluorescence Studies of Ni_{0.5-x}Mg_{0.5}Cu_xFe₂O₄ Nanoparticles

Pradeep Chavan (✉ cpajju@gmail.com)

S B Arts and K C P Science College <https://orcid.org/0000-0002-1964-4020>

Original Article

Keywords: Auto combustion technique, ferrite nanoparticles, FTIR, UV-Visible, Fluorescence and energy band gap

Posted Date: February 3rd, 2021

DOI: <https://doi.org/10.21203/rs.3.rs-174488/v1>

License:  This work is licensed under a Creative Commons Attribution 4.0 International License.

[Read Full License](#)

Version of Record: A version of this preprint was published at Journal of Fluorescence on April 23rd, 2021. See the published version at <https://doi.org/10.1007/s10895-021-02735-y>.

Abstract

The present study focused on the structural, morphological, optical and fluorescence properties of Ni_{0.5-x}Mg_{0.5}Cu_xFe₂O₄ (x = 0.0, 0.1, 0.3 and 0.5) nanoparticles synthesized by using auto combustion technique. The structural formation of the ferrite nanoparticles were confirmed by FTIR spectroscopic study. From FTIR spectra of the synthesized ferrite nanoparticles, metal ions are situated in two different sub lattices i.e. tetrahedral (A-site) and octahedral (B-site) in ferrites. The surface morphology and grain size of Cu substituted Ni-Mg ferrite nanoparticles were estimated from the micrographs of atomic force microscopy (AFM); the maximum grain size 54.69 nm was obtained. Spectra of UV-Visible absorption of the synthesized ferrite nanoparticles were carried-out by using UV-Vis spectrophotometry; the maximum absorption was observed at 418 nm. The energy band gap of ferrite nanoparticles has been estimated using UV-Vis absorption spectra; the energy band gap 3.50 eV was obtained. From the fluorescence emission spectroscopy of synthesized ferrite nanoparticles, the ferrite samples emit red colour in the region of 680 nm.

Introduction

Current advances in the field of material science enabled the community of research scientists to prepare and test the nano-scaled materials with different sizes, shapes and composition in favor of their applicability in the miscellaneous applications [1]. The ferrite nanoparticles with spinel structure play extensively an important role in the development of fundamental research in technological applications owing to their distinctive structural, electrical, optical and fluorescence properties. Synthesis of ferrite nanoparticles and study of their physical properties is the significant part of research in the present decade. The use of appropriate preparation technique and proper analysis of several physical properties by using various characterization techniques can lead to the applications of ferrite nanoparticles in various electronic technology and devices [2]. Thus, ferrites at the nano-scale acquire the noticeable physical and chemical properties than their bulk forms. Therefore, these noticeable and extraordinary properties of the nanoparticles lead to the applicability of ferrites in diverse fields ranging from electronics industry to the biomedical field. Apart from its optical, magnetic and electric properties, ferrite materials find wide applications in heterogeneous catalysis and in sensor technology, microwave control components such as isolators, circulators, phase shifters, high density recording devices and magnetic technologies, etc [3]. The consequence of molecular structure and motion of nanomaterials on the photochemical and photophysical properties of substituted ferrite nanoparticles have different modes of applications such as optoelectronics, optical data storage media and photonics, and also useful in thermal coagulation therapy; were tumours are locally heated by the use of alternating magnetic field [4]. In the recent years, ferrite nanomaterials attracted many researchers because of their various kinds of properties especially optical and fluorescence properties. Thus, the structural and optical properties of doped ferrite nanoparticles can be tuned by the type and amount of substituting elements chosen. Along with the nano-scaled materials, ferrite nanoparticles prove themselves as gifted materials for different practical device applications owing to their dual natured optical, electrical and magnetic properties [5].

In the present report, synthesis of $\text{Ni}_{0.5-x}\text{Mg}_{0.5}\text{Cu}_x\text{Fe}_2\text{O}_4$ ferrite nanoparticles by using auto combustion method is carried out. We reported the study of spectroscopic properties like UV-Visible absorption spectroscopy, fluorescence emission spectroscopy and surface morphological studies of the synthesized ferrite nanoparticles.

EXPERIMENTAL DETAILS

Analytical reagent grade materials of high purity metal nitrates like $\text{Ni}(\text{NO}_3)_2$, $\text{Mg}(\text{NO}_3)_2$, $\text{Cu}(\text{NO}_3)_2$ and $\text{Fe}(\text{NO}_3)_3$ are taken in a stoichiometric percentage and dissolved in 50 ml deionized water for standardized mixture. 10% of PVA solution was mixed with hot sucrose solution and stirred on the magnetic stirrer for the clear solution. All the prepared solutions were mixed together and then heated on the magnetic stirrer at the appropriate temperature until NO_2 vapours vanished completely and form gelatinous mixture. This mixture was heated on the gas burner until it burns like live charcoal undergoing corrosion reaction for the configuration of ferrite nanoparticles in powder form. The powder was presintered at 600°C for 8 hrs in the muffle furnace and cooled to room temperature. 2% of PVA was added to this powder which acts as a binding agent and then hard-pressed into the form of pellets using the hydraulic press of 5 tons/inch². The pellets were final sintered at 800°C for 10 hrs and furnace cooled to room temperature.

Results And Discussion

FTIR Spectroscopy

The victorious manufacture of spinel nature and the presence of supplementary functional entities in synthesized Cu substituted Ni-Mg ferrite samples were studied by the gifted FTIR (Fourier transform infrared spectroscopy). FTIR spectroscopy is an important tool to identify the stretching and bending vibrations of tetrahedral and octahedral complexes of ferrite nanoparticles. IR absorption bands are the common feature of spinel type ferrite materials. FTIR spectra of synthesized $\text{Ni}_{0.5-x}\text{Mg}_{0.5}\text{Cu}_x\text{Fe}_2\text{O}_4$ ferrite nanoparticles were shown in Fig. 1. The spectra of transmittance with respect to wavenumber were recorded in the range from 400 cm^{-1} to 4000 cm^{-1} . The absorption spectra confirmed the phase formation of cubic spinel structure and also elucidate the positions of cations in the crystal structure with oxygen ions as well as their vibrational modes [6].

These IR absorption bands represent the various ordering positions and structural properties of ferrite nanoparticles. The metal cations present in ferrite nanoparticles are situated in two different sub-lattices, i.e. tetrahedral (A-sites) sites and octahedral (B-sites) sites as stated by the oxygen ion nearest neighbours in the geometric configuration [7]. The sample shows two prominent absorption bands ν_1 and ν_2 in the range of 590 cm^{-1} and 428 cm^{-1} respectively. The absorption band around 590 cm^{-1} (ν_1) corresponds to intrinsic stretching vibration of metal cations at the tetrahedral site, while the band around 428 cm^{-1} (ν_2) corresponds to metal cations at the octahedral sites [8].

Table 1

FTIR absorption bands, UV-Vis absorption wavelength, energy band gap and fluorescence excitation wavelength of the Cu substituted Ni-Mg ferrite nanoparticles

x content	Absorption bands (cm ⁻¹)		Absorption Wavelength (nm)	Energy band gap (eV)	Excitation Wavelength (nm)
	ν_1	ν_2			
0.0	590	423	411	3.50	679
0.1	588	426	413	3.22	678
0.3	588	428	416	3.10	678
0.5	588	428	418	2.82	680

Thus, the position of absorption bands ν_1 and ν_2 are expected at around 600 cm⁻¹ and 400 cm⁻¹ due to the difference between Fe³⁺-O²⁻ distance of A-B site. Therefore, the band frequency ν_2 is less as compared to the ν_1 band; it was due to the fact that dimension of A-site is less compared with the dimension of B-site [9]. The absorption band ν_2 is shifted slightly to higher frequency side because of the addition of Cu²⁺ ions and attributed to the increasing in bond length of B-site. This suggests that Cu²⁺ ions occupied B-site. The presence of Fe²⁺ ions causes the splitting of absorption bands due to local lattice deformation caused by Jahn-Teller effect [10].

ATOMIC FORCE MICROSCOPY

Microscopic observations can be available for monitoring the variation in surface morphology and microstructure of ferrite nanoparticles. Surface morphology and grain size of Ni_{0.5-x}Mg_{0.5}Cu_xFe₂O₄ nanoparticles were studied. Nanosurf Easyscan2 software is a tool utilized to estimate the grain size directly from the scanned image of the samples. Surface of the sample was scanned in a raster pattern by noncontact mode using AFM shown in Fig. 2. The grain size of the synthesized Ni_{0.5-x}Mg_{0.5}Cu_xFe₂O₄ nanoparticles of about 54.69 nm was observed. It is to be noted that the grain size increases with increasing copper concentration in Ni-Mg ferrite nanoparticles; it was due to the grain growth and variation in ionic radii of the metal cations [11]. As the grains of ferrites grow larger, the grains boundary becomes more obvious and the pores escape from inside the grain along with grain boundaries easily. These results in most of the remnant pores remain in grain boundaries and grains grow to be denser and homogeneous. As a result, many pores become isolated from grain boundaries, and diffusion distance between the pores and grain boundary becomes large [12].

UV-VISIBLE ABSORPTION SPECTROSCOPY

Semiconducting ferrite nanoparticles which have absorption coefficient (α) and energy band gap (E_g) are the major optical features which specify the ability to use for optoelectronic applications. The absorption

coefficient (α) near the band edge shows an exponential upon photon energy usually obeying the expression as follows [13],

$$(\alpha h\nu)^2 = A (h\nu - E_g)^m$$

1

where α is the absorption coefficient, h is the Plank constant, and ν is the frequency of the incident radiation, E_g is the optical energy band gap, m is the nature of transition band gap (i.e. $m = 1/2$ for indirect and 2 for direct band gap materials), A is a constant of independent energy and $h\nu$ is photon energy.

Copper substituted Ni-Mg ferrite nanoparticles were analysed by using diffused UV-Visible reflectance spectroscopy to study their optical properties. Figure 3(a) shows UV-Visible absorption spectra with respect to wavelength of $\text{Ni}_{0.5-x}\text{Mg}_{0.5}\text{Cu}_x\text{Fe}_2\text{O}_4$ ferrite nanoparticles and it shows a maximum wavelength at 418 nm. It is to be noted that absorbance of copper substituted Ni-Mg ferrite nanoparticles ranging from 200–450 nm indicating the absorption of band edge has been broadened to region of visible light. [14] The absorbance characteristics of the nanostructured materials depend upon the number of factors such as energy band gap and surface roughness. Generally, energy band gap refers to the energy (eV) difference between valence band and conduction band. If the valence band is full of electrons and the conduction band is empty, then electrons cannot flow inside the materials; however, if some electrons transfer from the valence band to the conduction band then current can flow throughout the material [15]. Therefore, the energy band gap is an important parameter that determines the electrical conductivity of the materials. Hence, energy band gap is defined as occurring at the intercept of the linear extrapolation with x-axis. The energy band gap of polycrystalline ferrites estimated using Tauc plot. The graph of $(\alpha h\nu)^2$ versus $h\nu$ was plotted for $\text{Ni}_{0.5-x}\text{Mg}_{0.5}\text{Cu}_x\text{Fe}_2\text{O}_4$ nanoparticles to estimate the value of energy band gap of the synthesized ferrite nanoparticles shown in Fig. 3(b). The energy band gap was determined using Tauc 16 and Davis-Mott model 17 by extrapolating the linear portion of the plot to $(\alpha h\nu)^2 = 0$ and we found the maximum energy band gap 3.50 eV. It is observed that the increase of energy band gap with increasing concentration of copper in Ni-Mg ferrite was due to increase in the lattice constant of the ferrite nanoparticles.

It is clear that all synthesized samples overcome with an absorption band in the whole range exhibited a fine absorption in the visible light region (200–450 nm). The absorption band observed at 418 nm is assigned to the characteristic absorption band of Cu-Ni-Mg ferrite nanoparticles. On substituting copper in Ni-Mg ferrites, the absorption band is shifted to higher wavelength which indicates a decrease in the energy band gap shown in Fig. 3(b) [18]. The fundamental absorption band that corresponds to excitation of an electron from valence band to conduction band can be used to determine the energy band gap of the synthesized ferrite nanoparticles.

Thus, it is also observed that the decrease of energy band gap with respect to ferrite concentration was

Loading [MathJax]/jax/output/CommonHTML/fonts/TeX/fontdata.js } localized d-electrons of Cu^{2+} ions and band

electrons of Ni-Mg ferrite nanoparticles [19]. Thus the narrow energy band gap with Cu doping could be due to the formation of sub-bands in between the energy band gap and merging of their sub-bands with the conduction band to form a continuous band. Therefore, this decrease in the energy band gap with increasing Cu content in Ni-Mg ferrites which may be associated with several parameters including crystallite size, structural parameter, carrier concentrations, presence of very small amount of impurities etc [20].

FLUORESCENCE STUDIES

The fluorescence spectra of synthesized ferrite nanoparticles were recorded to investigate the luminescence properties and also to obtain the information on energy band gap with the relative energetic position of sub-band gap defect. The Fluorescence emission spectra of $\text{Ni}_{0.5-x}\text{Mg}_{0.5}\text{Cu}_x\text{Fe}_2\text{O}_4$ nanoparticles were shown in Fig. 4. It is observed that for the excitation wavelength of 418 nm, the ferrite samples emit red colour in the region of 680 nm [21]. This property of emission was due to the NO_2 and Nitrate groups present in ferrite nanoparticles. The cationic molecules weakly fluorescent in deionized water, when nitrates interact with the poly nucleotides then the fluorescence intensity increases [22]. The increasing copper concentration in $\text{Ni}_{0.5-x}\text{Mg}_{0.5}\text{Cu}_x\text{Fe}_2\text{O}_4$ nanoparticles results in the shifting of peak towards red region (> 680 nm) and fluorescence band became broaden can be ascribed to the formation of aggregated species [23].

Hence, the photo-induced electron transfer reaction is occurred mainly from a donor to an acceptor and it can be utilized for optical devices and optical storage applications etc [24]. This fluorescent behaviour of $\text{Ni}_{0.5-x}\text{Mg}_{0.5}\text{Cu}_x\text{Fe}_2\text{O}_4$ nanoparticles show gradually improved emission property which suggests that the enhancement of aggregation-induced fluorescence emission [25]. Thus, the emission characteristics of copper substituted Ni-Mg ferrite nanoparticles are governed by the defect controlled processes. It is also observed that doping of copper in Ni-Mg ferrites increases the fluorescence intensity with an increase in x values of copper. In spite of the fact that the defect controlled processes in all ferrite samples, the increase in the fluorescence intensity which was due to the increase in the distance between dopant (activator) and array [26]. Therefore, the defect center acts as trap levels and role of Cu^{2+} activators in increasing the intensity of fluorescence in the copper doped Ni-Mg ferrites play a dominant role in the emission processes [27].

Conclusion

The ferrite nanoparticles were synthesized by using auto combustion method. FTIR absorption spectra confirmed the formation of cubic spinel structure and also elucidate the positions of cations in the crystal structure with oxygen ions as well as their vibrational modes. The IR absorption bands represent the various ordering positions and structural properties for the different compositions of ferrites. The grain size of $\text{Ni}_{0.5-x}\text{Mg}_{0.5}\text{Cu}_x\text{Fe}_2\text{O}_4$ nanoparticles was determined from AFM study; the maximum grain size 54.69 nm was obtained. All synthesized samples overcome with an absorption band in the whole range (Loading [MathJax]/jax/output/CommonHTML/fonts/TeX/fontdata.js n). The absorption band observed at 418 nm is

assigned to the characteristic absorption band of Cu-Ni-Mg ferrite nanoparticles. From the fluorescence emission spectroscopy of synthesized ferrite nanoparticles, the fluorescent behaviour of $\text{Ni}_{0.5-x}\text{Mg}_{0.5}\text{Cu}_x\text{Fe}_2\text{O}_4$ nanoparticles show gradually improved emission property which suggests that the enhancement of aggregation-induced fluorescence emission.

Author Declarations

Declarations

Funding:

Author declares that this research work has no funding sources.

Conflicts of interest/Competing interests:

Author hereby declare that the research article entitled "Facile Synthesis, Diffused Reflectance Spectroscopy & Fluorescence Studies of $\text{Ni}_{0.5-x}\text{Mg}_{0.5}\text{Cu}_x\text{Fe}_2\text{O}_4$ Nanoparticles" have been submitted is not published elsewhere and not yet communicated in any of the journals. Author declares that there is no conflict of interest.

Ethics approval:

Author approves the submission of research article to Journal of Fluorescence.

Consent to participate:

Author approves the consent to participate.

Consent for publication:

Author approves the consent for publication of this article into journal of fluorescence.

Availability of data and material/ Data availability:

Data will be available on request.

Code availability: Not Applicable

Authors' contribution: Not Applicable

References

[1] Q. A. Pankhurst, J. Connolly, S. K. Jones, and J. Dobson, J. Phys. D. Appl. Phys. 36

(2003) 167.

- [2] J. Kulikowski, J. Magn. Magn. Mater 41 (1990) 56.
- [3] M. A. El Hiti, J. Phys. D. Appl. Phys. 29 (1999) 501.
- [4] A. Largeteau, J. M. Reau and J. Raves, Phys. Stat. Sol. (a). 111 (1990) 627.
- [5] A. M. Abdeen, J. Magn. Magn. Mater. 192 (1999) 121.
- [6] C. G. Koops, Phys. Rev. 83 (1951) 121.
- [7] Pradeep Chavan, L.R. Naik, P.B. Belavi, Geeta Chavan, C.K. Ramesha, and R.K. Kotnala, J. Elect. Mater. 46 (2017) 188.
- [8] V. R. K. Murthy and J. Sobhanadri, Phys. Stat. Sol. (a). 3 (1976) 647.
- [9] M. Naeem, N. A. Shah, I. H. Gul, and A. Maqsood, J. Alloys Compd. 487 (2009) 739.
- [10] M. A. Gabal and Y. M. Al Angari, Mater. Chem. Phys. 118 (2009) 153.
- [11] P. B. Belavi, G. N. Chavan, L. R. Naik, R. Somashekar, and R. K. Kotnala, Mater. Chem. Phys. 132 (2012) 138.
- [12] T. J. Shinde, A. B. Gadkari, and P. N. Vasambekar, Mater. Chem. Phys. 111 (2008) 87.
- [13] R.D. Waldron, Phys. Rev. 99 (1955) 1727.
- [14] Pradeep Chavan, L.R. Naik and R.K. Kotnala, J. Magn. Magn. Mater. 433 (2017) 24.
- [15] A. C. F. M. Costa, R. H. G. A. Kiminami, P. T. A. Santos, J. F. Silva J. Mater. Sci. 48 (2013) 172.
- [16] N. M. Mahmoodi, J. Taiwan Inst. Chem. Eng. 44 (2013) 322.
- [17] R. S. Gaikwad, S.-Y. Chae, R. S. Mane, S.-H. Han, and O.-S. Joo, Int. J. Electrochem. 2011 (2011) 1.
- [18] R. S. Devan and B. K. C. Y D Kolekar and, J. Phys. Condens. Matter 18 (2006) 9809.
- [19] E. J. W. Verwey, F. de Boer, and J. H. van Santen, J. Chem. Phys. 16 (1948) 1091.
- [20] Pradeep Chavan, L.R. Naik, P.B. Belavi, Geeta Chavan and R.K. Kotnala. J. Alloy.

[21] S. O. Aisida .et al. J. Macromol. Scienc. B. DOI: 10.1080/00222348.2020.1713519

[22] S. Wang. et al. J. Light. Elect. Optic. 185 (2019) 301.

[23] S. Debnath, R. Das, J. Molecul. Struct. 1199 (2020) 127044.

[24] Pradeep Chavan and L R Naik, Phys. Stat. Solid. A. 1700077 (2017) 1.

[25] P. Thakur, et al. J. Magn. Magn. Mater. 479 (2019) 317.

[26] Souvanik Talukdar. et. al. RSC. Adv. 8 (2018) 38.

[27] A. Shokri et al. Ceramic. International. 44 (2018) 22092.

Figures

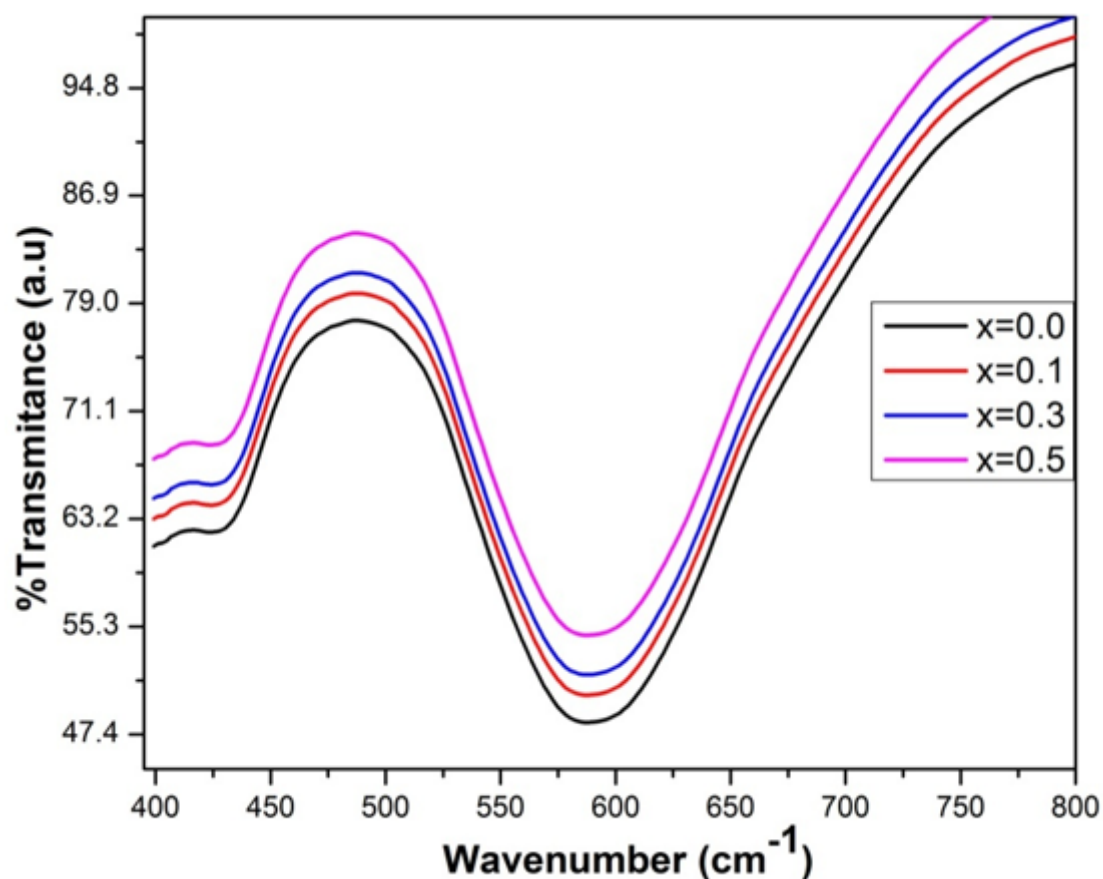


Figure 1

FTIR Spectra of Ni_{0.5-x}Mg_{0.5}Cu_xFe₂O₄ ferrite nanoparticles

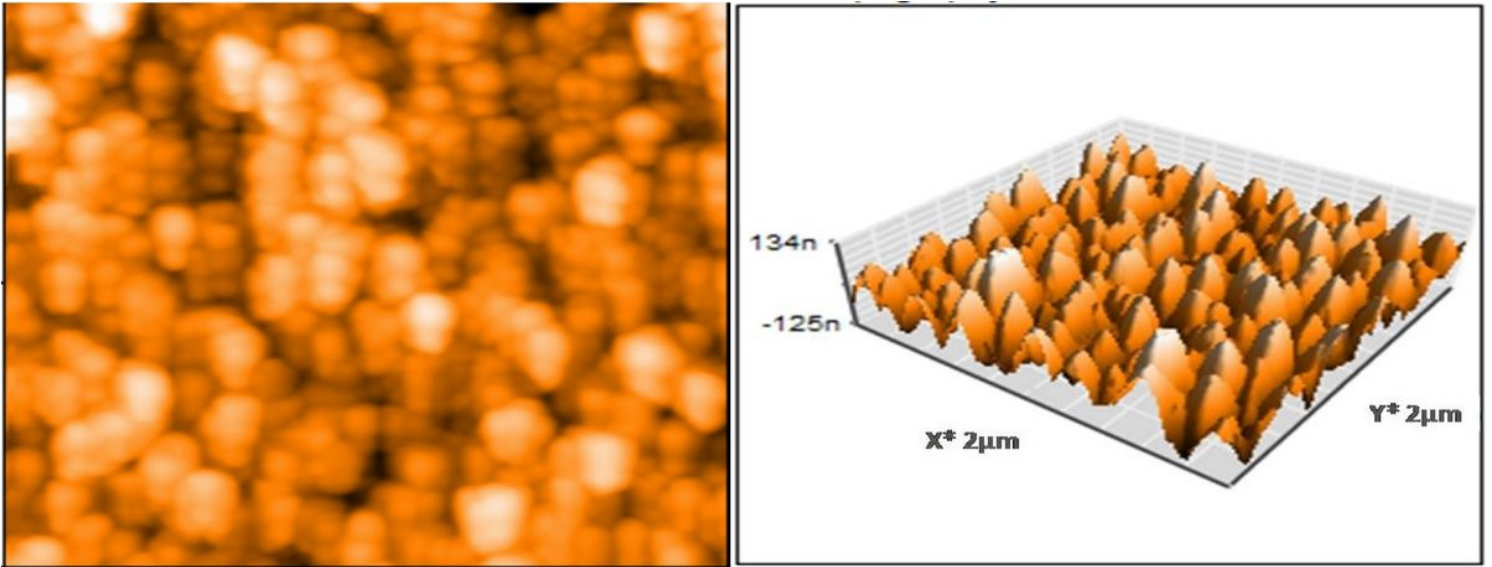


Figure 2

Surface morphological study of $\text{Ni}_{0.5-x}\text{Mg}_{0.5}\text{Cu}_x\text{Fe}_2\text{O}_4$ ferrite nanoparticles and 3D view of the ferrite samples

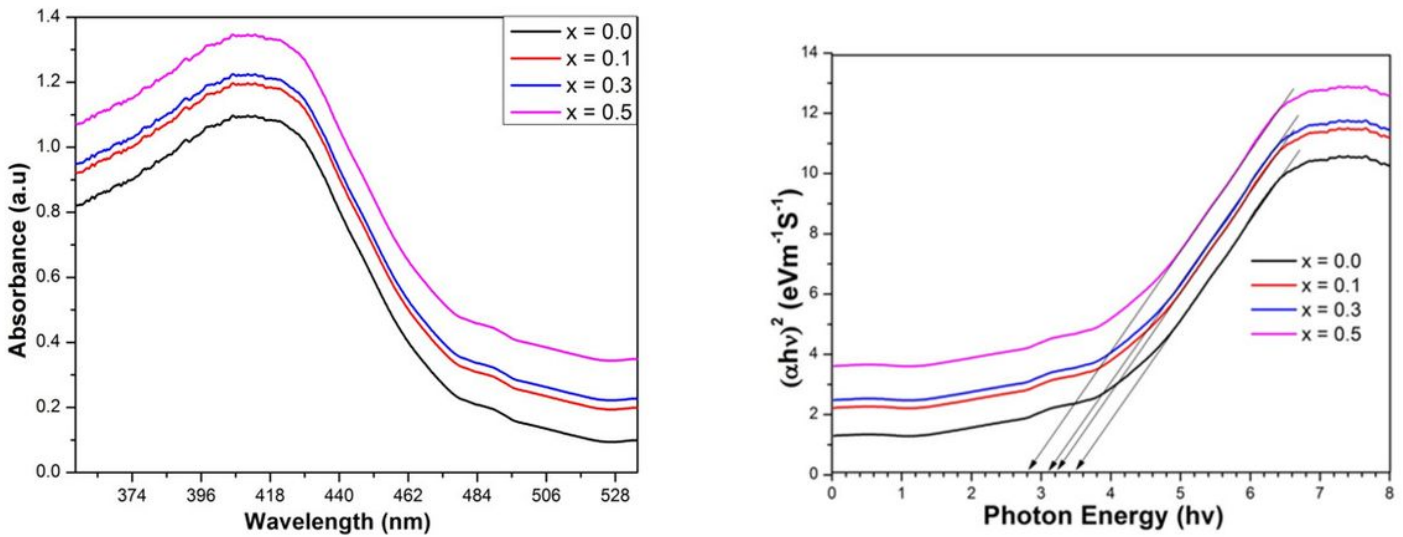


Figure 3

Left (a) UV-Visible absorption spectra of $\text{Ni}_{0.5-x}\text{Mg}_{0.5}\text{Cu}_x\text{Fe}_2\text{O}_4$ ferrite nanoparticles. Right (b) Spectra of energy band gap of $\text{Ni}_{0.5-x}\text{Mg}_{0.5}\text{Cu}_x\text{Fe}_2\text{O}_4$ ferrite nanoparticles

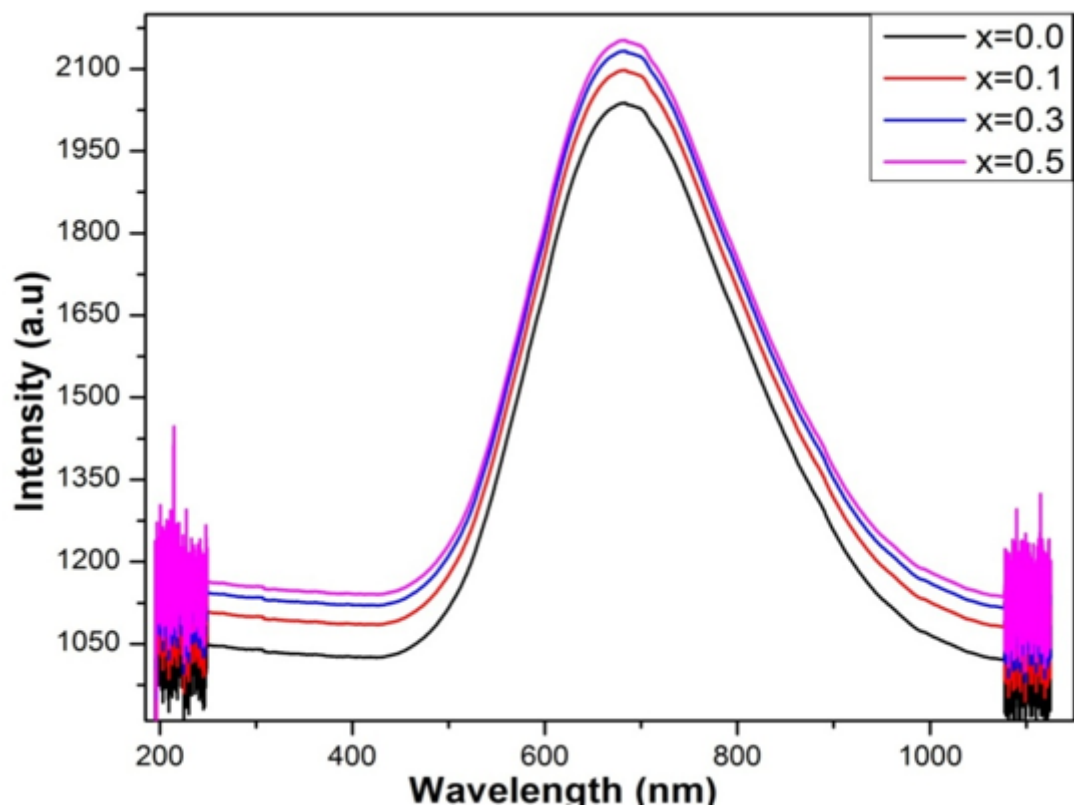


Figure 4

Fluorescence emission spectra of $\text{Ni}_{0.5-x}\text{Mg}_{0.5}\text{Cu}_x\text{Fe}_2\text{O}_4$ ferrite nanoparticles